Journal of Photochemistry and Photobiology A: Chemistry 218 (2011) 76–86

Contents lists available at ScienceDirect

Journal of Photochemistry and Photobiology A: Chemistry

journal homepage: www.elsevier.com/locate/jphotochem

Study on intramolecular charge transfer fluorescence properties of trans-4-[4′-(N,N′-dimethylamino)styryl]pyridine: Effect of solvent and pH

M. Sowmiya, Amit K. Tiwari, Sonu, Subit K. Saha*

Department of Chemistry, Birla Institute of Technology and Science, Pilani 333 031, Rajasthan, India

ARTICLE INFO

Article history:
Received 20 August 2010
Received in revised form 4 November 2010
Accepted 8 December 2010
Available online 21 December 2010

Keywords:
ICT/TICT fluorescence
4-DMASP
Donor twisting
Acceptor twisting
Excited state dipole moment
Acidity constant

ABSTRACT

Photophysical characterization of a molecule, trans-4-[4′-(N,N′-dimethylamino)styryl]pyridine (4-DMASP) containing donor and acceptor moieties has been done experimentally as well as theoretically. Upon single excitation a charge-transfer state with high dipole moment is formed through rapid relaxation of a locally excited (LE) state in polar medium. A complete charge transfer process occurs as a result of twisting of donor group with respect to the acceptor part of the molecule resulting in the highly stabilized twisted state in polar medium giving fluorescence from LE state as well as from twisted state. However, in a nonpolar solvent emission occurs explicitly from a LE state. Hydrogen bond donor ability of solvents rather than dipolar interactions contributes more to the stability of ground state. However, dipolar interactions have greater contribution towards the stability of an excited state. All such interactions have higher contribution towards the stability of excited state than that of ground state. Very low fluorescence quantum yield in water is because of high rate of nonradiative processes as a result of high degree of stabilization of charge transfer state thereby making closer proximity of this state to triplet as well as ground charge transfer states. Monocation of 4-DMASP formed due to the protonation of pyridine nitrogen atom is more stable than neutral and dication species at ground as well as excited states because of greater extent of flow of charge from donor to acceptor part in monocation. Basicity of pyridine nitrogen atom being greater at excited state than that in ground state results in higher extent of pulling of charge from donor to acceptor part of monocation at excited state. Theoretical calculations suggest donor twisting as a possible path for creation of a charge transfer state rather than acceptor twisting. Excited state dipole moment value obtained from theoretical calculation corroborates well with the value determined experimentally. Theoretical calculation suggests no cis–trans photoisomerization in the ground state as well as excited state at room temperature.

1. Introduction

From the time the dual fluorescence of dimethylaminobenzonitrile (DMABN) in polar solvents reported by Rotkiewicz and Grabowski [1,2] for its twisted intramolecular charge transfer (TICT) phenomenon, the molecular systems with similar charge transfer fluorescence properties have found their potential applications in photoelectronic devices [2], chemical sensor [3], nonlinear optical properties [4], probing molecule induced nanotubular suprastructures [5] and photobiological process [6]. Upon excitation, molecular systems with donor and acceptor connected by a single bond may exist as intramolecular charge transfer (ICT) or TICT state [7–12]. Many such molecules show dual fluorescence where a short wavelength emission arises from the locally excited (LE) state whereas the ICT state is responsible for the emission at longer wavelength in polar and/or viscous medium [1,7–12]. In many cases complete charge transfer occurs as a result of twisting of donor with respect to the acceptor part of the molecule resulting in the highly stabilized TICT state in polar medium giving fluorescence from LE as well as TICT state upon single excitation [8,9,13].

Among the different TICT molecules reported so far, pyridine derivatives deserves important role in wide areas such as in the determination of cell microviscosity [14], chemiluminescence [15], fluorescent sensor [4], and silane sol–gel transition studies [16] to name a few.

Bruni et al. [17] studied the solvatochromism of trans-4-[4′-(N,N′-dimethylamino)styryl]pyridine (4-DMASP) [Scheme 1] and dimethylamino-1,10-phenalthroline (DAPHEN) to determine the

---

* Corresponding author. Tel.: +91 1596 515238; fax: +91 1596 244183.
E-mail addresses: sksaha@bits-pilani.ac.in, subitksaha@gmail.com (S.K. Saha).

1010-6030/$ – see front matter © 2010 Elsevier B.V. All rights reserved.
doi:10.1016/j.jphotochem.2010.12.006

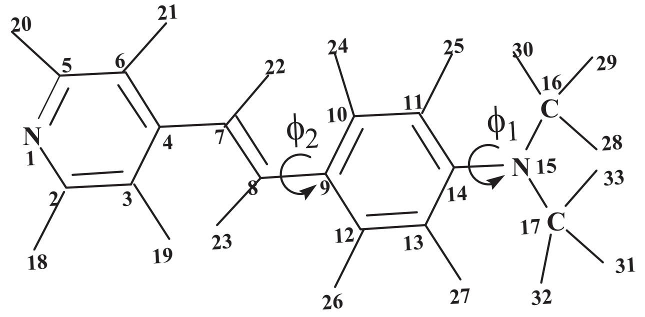

Scheme 1. Structure of 4-DMASP.

quadratic hyperpolarizability, β of dipolar molecules. In their paper they reported the charge transfer behavior of 4-DMASP to rationalize the more polar excited state than the ground state. In addition, Wang et al. [18], reported excited state deprotonation (ESDP) process of 4-DMASP by analyzing the behavior of it in chloroform in different acidic concentrations. They proposed intramolecular charge transfer (ICT) character for a red shift in emission spectra with an increase of solvent polarity. As this molecule is having dimethylamine group which is connected with a styrylpyridine with a single bond, it can very well act as donor–acceptor system. Sensitivity of fluorescence properties of a derivative of 4-DMASP towards viscosity of medium has made it useful as a fluorescent probe for cell microviscosity [14].

In this paper, we have reported effect of solvent and hydrogen ion concentration on fluorescence emission properties of 4-DMASP. Dependence of large Stokes shifted fluorescence band on the polarity of medium supports emission from ICT state. To investigate the origin of charge transfer state, quantum chemical AM1-SCI (singly excited configuration interaction) calculations have been carried out. Recently, Chakraborty et al. [19] have reported dual fluorescence of a donor–acceptor system, trans-3-(4-monomethylamino-phenyl)-acrylic acid (*t*-MMPAA) giving normal fluorescence from LE state and large Stokes shifted fluorescence from twisted excited state of charge transfer character. The theoretical calculations performed on the molecule raised the possibility of having stable twisted excited state through two twisting coordinates: one along donor and other along the acceptor twisting path. However, their molecular orbital calculation showing HOMO as localized nitrogen lone pair orbital suggested occurrence of TICT state through donor-twisting path. Present calculation on 4-DMASP suggests that charge-transfer state is created through the relaxation of LE state in polar medium only after twisting of donor part of the molecule with respect to acceptor part. High dipole moment of twisted conformation results in stabilization of TICT state in polar solvents giving highly Stokes shifted fluorescence bands.

Wang et al. [18] have reported basicity difference between the excited state and the ground state (ΔpK_a) of neutral and monocation species of 4-DMASP using Förster cycle method. In the present work, we have determined ground state acidity constant (pK_a) of dication–monocation equilibrium and have shown that excited state equilibrium between the same species cannot exist because of faster rate of emissions of species compared to the rate of proton transfer between them.

Although, charge-transfer nature of fluorescence emissions of 4-DMASP and its derivatives in various types of polar solvents (protic and aprotic) have been indicated by different groups [14,18], but present study find out the individual contribution of dipole–dipole interactions, hydrogen bond donor ability and acceptor ability of solvents towards the stability of ground state as well as excited state of the molecule by the solvatochromic comparison method (SCM) proposed by Kamlet et al. [20].

2. Experimental

2.1. Materials and methods

4-DMASP was procured from Sigma–Aldrich chemical company, WI, USA and was recrystalized three times from a mixture of ethanol and a small percentage of n-hexane. All the solvents used were of spectroscopic grade and procured from Spectrochem Company, India. Triple distilled water was used for the preparation of the aqueous solutions. Dilute sulfuric acid and sodium hydroxide solutions were used to adjust the pH of the prepared aqueous solutions. A stock solution of 4-DMASP (5×10^{-4} M) was prepared in pure methanol to record the UV–visible absorption and fluorescence spectra of it in pure solvents; 0.1 mL of this solution was poured in a 10 mL volumetric flask and left for a few hours for complete evaporation of methanol and then the compound was dissolved in respective solvents to make final volume of 10 mL. The concentration of 4-DMASP in all the experimental solutions used for spectroscopic measurements was 5×10^{-6} M. The fluorescence quantum yields were determined with respect to that of quinine sulfate in 0.1N H_2SO_4 (0.55). The absorption spectra were recorded using a Hitachi U-2900 UV–visible spectrophotometer. Fluorescence measurements were performed using Horiba Jobin Yvon Fluoromax-4 scanning spectrofluorimeter. Eutech PC 510 pH meter was used to adjust the pH of aqueous solutions. All spectroscopic measurements were done at room temperature, $25 \pm 1\,^{\circ}$C.

2.1.1. Solvatochromic comparison method (SCM)

This method was proposed by Kamlet et al. [20] provides information about the individual contribution of different solvent effects. This multiparamateric approach separates the dielectric effects of solvents (π^*), hydrogen-bond donor ability (α), and hydrogen-bond acceptor ability (β) of the solvents on the spectral properties. The equation describing these effects is:

$$E = E^0 + c\pi^* + a\alpha + b\beta \tag{1}$$

where a, b and c are the coefficients and E^0 is the spectral maxima independent of solvent effects. The values of π^*, α and β of different solvents have been taken from the report of Kamlet et al. [20]. The values of E are absorption/fluorescence band maxima in terms of cm^{-1}.

2.1.2. Quantum chemical calculations

Hyperchem package Version 6.01 (Hypercube Inc., Canada) has been used for the theoretical calculations. The ground state (S_0) geometry of the compound was optimized by AM1 method [21–24]. AM1-SCI was performed to get the energy (E_g) and dipole moment in the ground state, the transition energies ($\Delta E_{i\to j}$), and dipole moments of different excited states. We have taken care of all the singly excited configurations within an energy window of 10.5 eV from the ground state. $\Delta E_{i\to j}$ corresponds to the excitation of an electron from the orbital φ_i (occupied in the ground state) to the orbital φ_j (unoccupied in the excited state). The total energy of the excited state (E_j) was then calculated as $E_j = E_g + \Delta E_{i\to j}$. The CI wavefunction has been used to generate *g* orbitals and one-electron density matrices, which were used to calculate the dipole moments of the excited states of the compound. The stabilization of different states due to solvation has been calculated from the solvation energies based on Onsager's theory [25]. Assuming that the solute molecule having a dipole μ_i in the ith electronic state is fully solvated, the solvation energy is given by

$$\Delta E_{\text{solv}} = \frac{2\mu_i^2(\varepsilon - 1)}{a^3(2\varepsilon + 1)} \tag{2}$$

where ε is the relative permittivity of the solvent and a is the cavity radius.

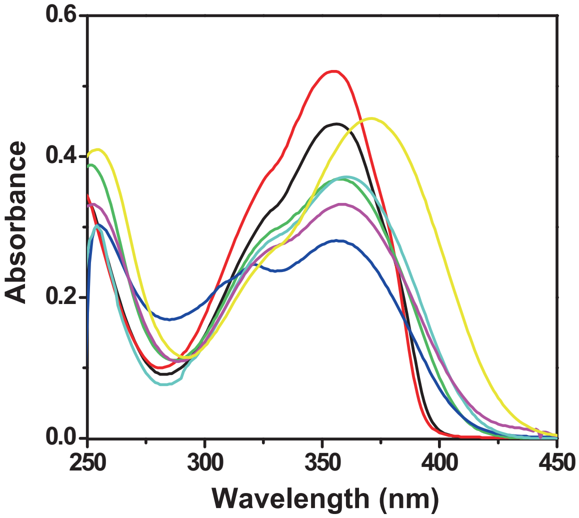

Fig. 1. Absorption spectra of 4-DMASP in different pure solvents at [4-DMASP] = 5 μM. Spectra correspond to cyclohexane (⬛), n-hexane (🟥), dioxane (🟩), ethylacetate (🟦), THF (🟦), acetonitrile (🟪) and methanol (🟨). (For interpretation of the references to color in this figure legend, the reader is referred to the web version of the article.)

3. Results and discussion

3.1. UV–visible absorption study of 4-DMASP

The UV–visible absorption spectra of 4-DMASP in pure solvents of different polarities are recorded and some representative spectra are shown in Fig. 1. As can be seen in the spectra, two absorption bands appear at ~330 nm and ~360 nm. These bands can be assigned to the transition to two different excited states from ground state.

Both the absorption peak maxima ($\lambda_{\max}^{ab}$) and the log $\varepsilon^{\max}$ values corresponding to lower energy band are given in Table 1. Although there is almost no shift of higher energy band, but the lower energy band is red shifted with increasing the polarity of the solvents. Similar observation has been reported by Chakraborty et al. [19] for the molecule, *t*-MMPAA. As for example, in comparison to lower energy absorption peak maximum appears at 356 nm in cyclohexane, the same appears at 372 nm in case of methanol as solvent. The red shift with increasing polarity of solvent indicates that the excited state is more polar than the ground state which is consistent with the charge transfer characteristics as a result of donation of electron from –N(CH$_3$)$_2$ group to the π^* system of the acceptor part of the molecule, 4-DMASP [17].

As absorption represents the transition from ground state to the Frank–Condon state, the observed red shift of lower energy band indicates the stabilization of Frank–Condon state or LE state [26]. The absorption data of lower energy band is also analyzed using the solvent comparison method proposed by Kamlet et al. [20]. The equation obtained from this approach with regression coefficient value 0.92 is as follows:

$$E\ \ (\text{cm}^{-1}) = 27,942.59 - 370.2\pi^* - 876.04\alpha - 103.21\beta \qquad (3)$$

The negative values of ‘*c*’, ‘*a*’ and ‘*b*’ indicate stabilization. The negative value of ‘*a*’ implies that the donation of lone pair of electrons of pyridine nitrogen atom to hydrogen-bonding solvents favors the pulling of electrons resulting in greater delocalization of lone pair of electrons of nitrogen atom of –N(CH$_3$)$_2$ with the π cloud of the ring [18,27]. This accounts for the above mentioned red shift in absorption band in protic solvents. Moreover, stabilization in hydrogen-bonding solvents also gives the clue that the basicity of pyridine nitrogen atom is higher than the basicity of the nitrogen atom of –N(CH$_3$)$_2$ group at ground state, because influence of hydrogen bonds to the absorption or emission spectra is although less than protonation but in the same direction [18]. The charge densities on pyridine nitrogen atom and nitrogen atom of –N(CH$_3$)$_2$ group at ground state are found to be −0.65 and −0.59, respectively obtained after performing geometry optimization ab initio calculation (RHF method and 6-31G** basis set) using Gaussian 98 software [28]. These values are consistent with the basicity of nitrogen atoms at ground state. The negative value of ‘*c*’ indicates stabilization due to dipolar interactions which attributes to the red shift of absorption band on increasing the polarity of the solvent as also observed in our previous work [27]. However, higher magnitude of ‘*a*’ compared to that of ‘*c*’ indicates that dipolar interactions offer minor contribution.

3.2. Fluorescence study of 4-DMASP

The fluorescence spectra of 4-DMASP are recorded in pure solvents of different polarities at λ_{ex} = 370 nm and some of them are shown in Fig. 2. Fluorescence peak maxima ($\lambda_{\max}^{fl}$), quantum yields and Stokes shift values are also tabulated in Table 1. The fluorescence band is structured in a nonpolar solvent as can be seen in

Table 1
Absorption peak maxima ($\lambda_{\max}^{ab}$), log $\varepsilon_{\max}$, fluorescence peak maxima ($\lambda_{\max}^{fl}$), fluorescence quantum yields (ϕ_f) and Stokes shift ($\bar{\upsilon}_{ss}$) of 4-DMASP in different solvents.

Solvent	$\lambda_{\max}^{ab}$ (nm)	log $\varepsilon_{\max}$ [a,b]	$\lambda_{\max}^{fl}$ [c] (nm)	$\bar{\upsilon}_{ss}$ (cm^{-1})	ϕ_f [d]
Cyclohexane	328, 356	4.95	418	4166	0.0079
n-Hexane	328, 355	5.02	417	4188	0.0079
Diethyl ether	326, 355	5.02	439	5390	0.0080
1,4-Dioxane	328, 358	4.87	441	5257	0.0097
THF[e]	328, 361	4.87	459	5914	0.0103
Ethylacetate	323, 357	4.75	451	5838	0.0125
DMF[f]	328, 365	4.84	486	6821	0.0157
DMSO[g]	385	4.84	502	6054	0.0146
Acetonitrile	327, 359	4.81	484	7194	0.0147
Isopropanol	327, 368	4.84	475	6121	0.0092
Ethanol	327, 370	4.85	487	6493	0.0106
Methanol	328, 372	4.96	497	6761	0.0088
Water (5% MeOH)	328, 373	4.95	510	7202	0.0030

[a] [4-DMASP] = 5 μM.
[b] Corresponding to longer wavelength band.
[c] λ_{ex} = 370 nm.
[d] λ_{ex} = 370 nm.
[e] Tetrahydrofuran.
[f] Dimethylformamide.
[g] Dimethylsulfoxide.

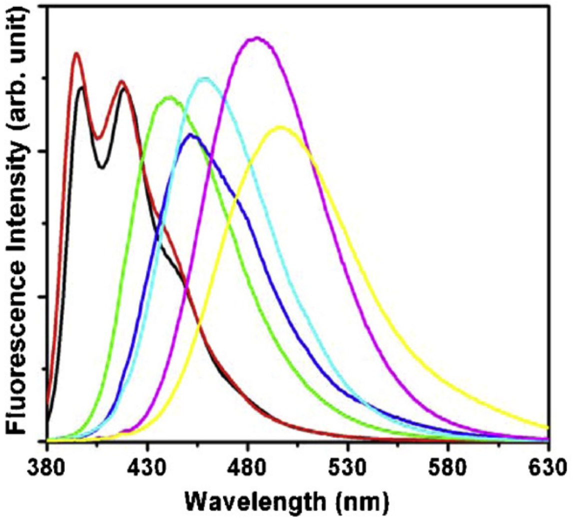

Fig. 2. Emission spectra of 4-DMASP in different pure solvents at [4-DMASP] = 5 μM. Spectra correspond to cyclohexane (⬛), n-hexane (🟥),dioxane (🟩), ethylacetate (🟦), THF (🟦), acetonitrile (🟪) and methanol (🟨) (λ_{ex} = 370 nm). (For interpretation of the references to color in this figure legend, the reader is referred to the web version of the article.)

Fig. 2 for cyclohexane. Therefore, emission can be assigned to be originated from the LE state in a nonpolar solvent. However, in polar aprotic and polar protic solvents broad structureless bands are noticed. There is a progressive significant bathochromic shift on increasing the polarity of the solvent, characteristics of a charge-transfer (CT) emission [19,29]. The progressive bathochromic shift of charge-transfer band on increasing the polarity of the solvent depicts that the fluorescence originates from a highly polar state. Fluorescence spectra are found to be independent of excitation wavelength as can be seen as supplementary material (Fig. S1) for λ_{ex} = 310 nm.

The excitation spectra in polar aprotic and polar protic solvents are dependent on the emission wavelengths giving excitation bands with peak maxima in the range of ~353 nm to ~375 nm in methanol as a representative solvent (Fig. 3). The excitation spectrum found at 353 nm progressively gets red shifted with increasing emission wavelength finally giving band with fixed wavelength at 375 nm. The excitation spectrum with peak maximum at 353 nm lies in the higher energy region of an absorption spectrum, whereas the same with peak maximum at 375 nm corresponds to the lower energy band in the same absorption spectrum. Similar types of excitation spectra were noticed in all other polar protic as well as polar aprotic solvents. Thus, emission wavelength dependent excitation spectra suggest that different excited state species are responsible for emission although the intensity of LE state fluorescence is very low in the present case. Contrary to the findings of Chakraborty et al. [19] for the molecule, *t*-MMPAA, in our case CT excited state may not be created only through singly LE species but also by the excitation of ground state CT species probably exists as a result of strong interactions between solute and solvent shell forming a possible complex between 4-DMASP and solvent [13,30–33]. As reported in the literature [13,27,34], the geometry of ground CT species is twisted as discussed later in theoretical calculation section.

To support further the existence of CT emitting states in addition to LE state, the fluorescence spectra of 4-DMASP have been recorded in different percentages of dioxane–water mixtures. One can see in Fig. 4 that with increasing the percentage of water in the mixture, fluorescence band gets red shifted with concomitant increase in intensity of band up to 56% of water in the mixture. The decrease in intensity starts after this with continuity in the bathochromic shift of the bands with further increasing content of water could be attributed to the stabilization of CT excited state thereby becoming closer to the triplet as well as ground twisted states [27,34]. The rates of intersystem crossing and internal conversion are expected to be increased because of this energetically closer proximity of CT excited state to the triplet state and ground twisted state, respectively. However, initial increase in quantum yield of fluorescence is as a result of progressive increase in the population of CT states with increasing polarity of the medium [27,29]. As expected, quantum yield increases reaches a maximum and then decreases with increasing polarity of the medium as shown in Fig. 4 (inset).

Although excitation spectra in polar protic and aprotic solvents are emission wavelength dependent, the same are independent in nonpolar solvents. Fig. 5 shows that an excitation spectrum in cyclohexane almost matching with the absorption spectrum

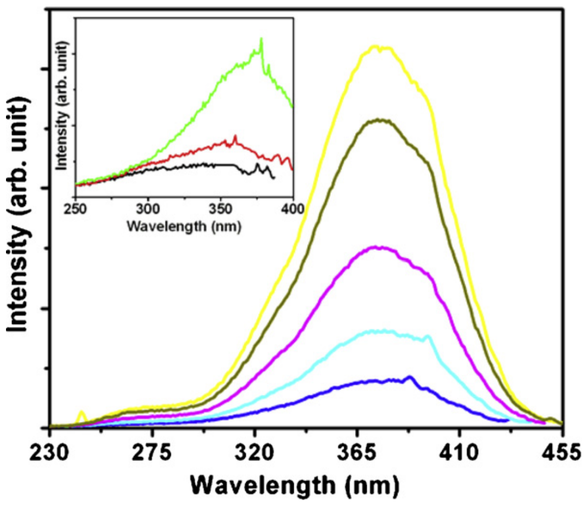

Fig. 3. Excitation spectra of 4-DMASP in methanol at different emission wavelengths. [Inset represents clear change in excitation spectra with respect to emission wavelength 400 (⬛), 415 (🟥) and 430 (🟩).] Spectra correspond to 440 (🟦), 450 (🟦), 460 (🟪), 490 (🟨) and 520 (🟫) nm emission wavelength. (For interpretation of the references to color in this figure legend, the reader is referred to the web version of the article.)

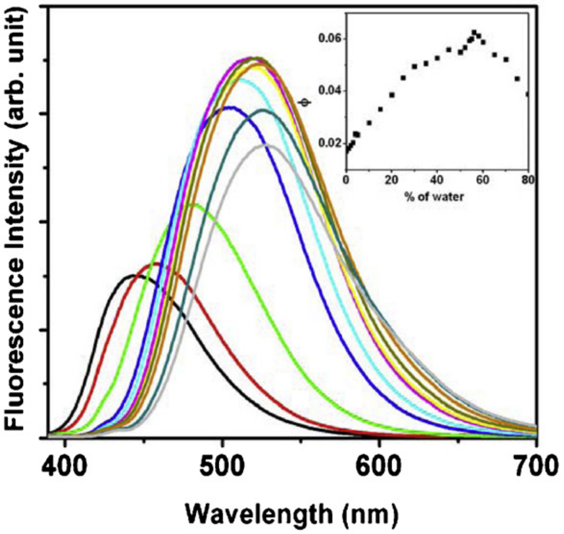

Fig. 4. Emission spectra of 4-DMASP in different percentages of dioxane–water mixtures (λ_{ex} = 375 nm). Spectra correspond to 100 (⬛), 98 (🟥), 90 (🟩), 70 (🟦), 60 (🟦), 50 (🟪), 46 (🟨), 42 (🟫), 35 (🟧) and 25 (🟩) and 20 (⬜) percent of dioxane in mixture. [Inset represents quantum yield of 4-DMASP as a function of percentage of water in mixture.] (For interpretation of the references to color in this figure legend, the reader is referred to the web version of the article.)

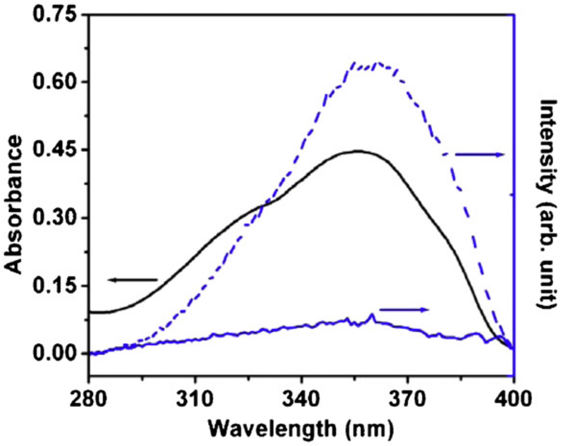

Fig. 5. Absorption (—) and excitation (▬ ▬ ▬) spectrum (λ_{em} = 470 nm) of 4-DMASP in cyclohexane and excitation (▬▬▬) spectrum of 4-DMASP in methanol (λ_{em} = 415 nm). (For interpretation of the references to color in this figure legend, the reader is referred to the web version of the article.)

with peak maxima at 357 nm. The excitation spectrum corresponding to the lower wavelength emission in methanol lies in the higher energy region of absorption spectrum also matches with the absorption spectrum in cyclohexane. This can be attributed to the fact that LE state is responsible for fluorescence at lower wavelength region. However, occurrence of fluorescence band with peak maxima at 497 nm in case of methanol which corresponds to an excitation spectrum in the higher wavelength region of absorption spectrum is depicting that the band is due to CT fluorescence. The presence of dimethylamino group connected by the flexible single bond to the benzene ring of styrylpyridine group can very well act as the donor–acceptor system as observed by different groups for similar probes [35,36]. This is also worthy to be mentioned here that upon a higher energy excitation to a LE state, a molecule whose geometry is similar to planar ground state follows a complete charge transfer process occurring as a result of twisting of donor, –N(CH_3)$_2$ group with respect to the acceptor part of the molecule connected by the flexible single bond (Scheme 1) resulting in the highly stabilized TICT state in polar medium giving fluorescence from LE state as well as from TICT state with corresponding excitation bands with peak maxima at ~353 nm and ~375 nm, respectively in case of methanol as solvent [Fig. 3] [8,9,13]. Excitation spectra taken in polar protic and aprotic solvents confirm fluorescence from two different emitting states, LE and CT although very low intensity of LE fluorescence is noticed. Low quantum yield of LE fluorescence and the pronounced solvent dependence of the charge transfer band of 4-DMASP have been attributed to rapid relaxation of the initially formed LE state to a charge-transfer (CT) state, similar to the photochemistry of different amino stilbenes [37].

SCM has also been applied to analyze the fluorescence data, which results into the following equation with regression coefficient value = 0.99:

$$E\ (\text{cm}^{-1}) = 23,947.98 - 4036.9\pi^* - 1990.9\alpha + 423.9\beta \qquad (4)$$

Negative values of '*c*' and '*a*' indicate stabilization whereas positive value of '*b*' indicates destabilization. The greater magnitudes of both '*c*' and '*a*' for excited state compared to that of ground state are in accordance with the fact that dipole–dipole interactions and hydrogen bond acceptor ability of molecule contribute more to the stabilization of excited state than that of ground state. The higher contribution of dipole–dipole interactions towards the stability of excited state is supported by high dipole moment of 4-DMASP (16.98 Debye) in the excited state (discussed later) than that in the ground state (6.86 Debye). The greater extent of charge transfer process from donor to acceptor part of such push–pull system at the excited state [18] in a solvent of hydrogen bond donor ability is responsible for another contributing factor for higher extent of stabilization of excited state. This is further supported by the values of charge densities on pyridine nitrogen atom and nitrogen atom of –N(CH_3)$_2$ group found to be −0.68 and −0.56 by excited state geometry optimization ab initio calculation (CI method and 6-31G** basis set). The charge density on pyridine nitrogen atom is higher whereas the same on nitrogen atom of –N(CH_3)$_2$ group is lesser at the excited state compared to that in the ground state. In this SCM calculation, data for water and DMSO as solvents are not included because of uncertainty of fluorescence peak maxima of broad band in water and existence of unusually high quantum yield of fluorescence in DMSO.

The difference between the dipole moments of 4-DMASP at excited and the ground states have been calculated by plotting the Stokes shift ($\bar{\nu}_{ab} - \bar{\nu}_{fl}$) against Δf using following Lippert–Mataga equation (Eq. (5)) [38]:

$$\bar{\nu}_{ab} - \bar{\nu}_{fl} = \left[\frac{2(\mu_e - \mu_g)^2}{hca^3}\right]\Delta f + \text{constant} \qquad (5)$$

where

$$\Delta f = \frac{\varepsilon - 1}{2\varepsilon + 1} - \frac{n^2 - 1}{2n^2 + 1} \qquad (6)$$

ε and n are dielectric constant and refractive index of a particular solvent, respectively, μ_g and μ_e are the ground state and excited state dipole moments, respectively, h Planck's constant, c the velocity of light, a the Onsager cavity radius. The cavity radius of 4-DMASP is taken as 4.81 Å calculated using RHF method with 6-31G** basis set by Gaussian 98 software. From the slope of the plot of Stokes shift against Δf (Fig. 6), the excited state dipole moment (μ_e) of 4-DMASP is calculated to be 16.98 Debye, where the ground state dipole moment (μ_g) of global minimum structure is 6.86 Debye obtained from ab initio calculation (RHF method and 6-31G** basis set). This high value of excited state dipole moment supports the charge transfer behavior of 4-DMASP in polar medium. The μ_e value of 4-DMASP calculated by Bruni et al. [17] by their proposed method was found to be 13.7 Debye. The difference in μ_e values could be because of choice of the value of a. In this work, this value has been calculated by running an energy calculation method specially given for producing an estimate value of a in Gaus-

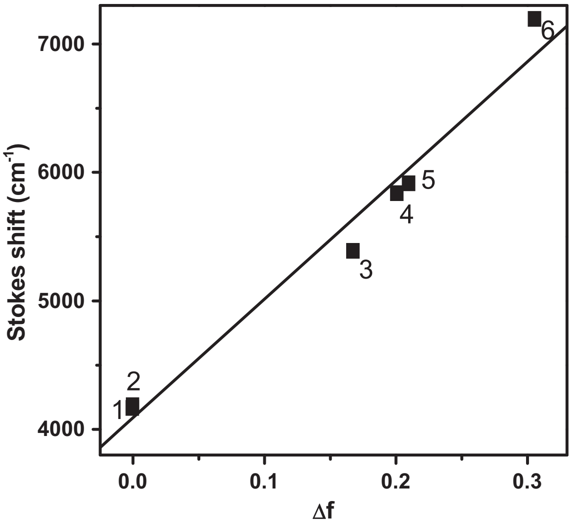

Fig. 6. Plot of Stokes shift of 4-DMASP vs. Δf in (1) cyclohexane, (2) n-hexane, (3) diethylether, (4) ethylacetate, (5) tetrahydrofuran and (6) acetonitrile.

Table 2
Excited singlet state lifetimes (τ), average singlet state lifetimes (τ_{avg}), preexponential factors (a), emission (λ_{em}) wavelengths, quantum yields (ϕ), radiative (k_f) and non-radiative (k_{nr}) rate constants of 4-DMASP in different solvents.

Solvent	λ_{em}[a] (nm)	τ (ps)	χ^2[b]	A	τ_{avg} (ps)	ϕ[c]	k_f (s^{-1})	k_{nr} (s^{-1})
Cyclohexane	418	53.9	1.10	–	–	0.0079	1.47×10^8	1.84×10^{10}
1,4-dioxane	441	58.6	1.10	–	–	0.0097	1.66×10^8	1.69×10^{10}
Ethylacetate	451	53.2	1.06	0.360	555.0	0.0125	2.25×10^7	1.78×10^9
		838.0		0.640				
Methanol	497	53.9	1.07	0.995	53.91	0.0088	1.63×10^8	1.84×10^{10}
		54.8		0.005				
Water (5% methanol)	510	51.5	1.10	–	–	0.0030	5.83×10^7	1.94×10^{10}

[a] λ_{ex} = 370 nm.

[b] χ^2 values have been given instead of the fit residuals for clarity and to save space.

[c] Standard deviation ±0.0001.

sian. This large change in dipole moment from ground to excited state is caused by the redistribution of atomic charges in excited state, which is only possible due to charge transfer from electron rich donor moiety to acceptor moiety as suggested for the probe 4-N,N-dimethylamino cinnamaldehyde [39].

3.3. *Effect of nature of solvents on excited singlet state lifetime*

Table 2 gives excited singlet state lifetimes, quantum yields, radiative and non-radiative rate constant values of 4-DMASP with corresponding excitation and emission wavelengths in two nonpolar solvents (cyclohexane and dioxane), one polar aprotic solvent (ethylacetate) and two hydrogen bonding solvents (methanol and water). In case of cyclohexane, dioxane and water decays are monoexponential. However, biexponential decays are noticed in ethylacetate and methanol. Mean (average) singlet state lifetime for biexponential iterative fitting have been calculated from the decay times and the pre-exponential factors (a_i) using the following equation [40]:

$$\tau_{avg} = a_1\tau_1 + a_2\tau_2 \tag{7}$$

Monoexponential decay in case of a nonpolar solvent is due to LE species, whereas LE and charge transfer species are responsible for biexponential decays in a polar solvent except in water where charge transfer species only decays. As LE species only decays in dioxane and cyclohexane and polarity of former is little higher than that of later, data in Table 2 might be indicating that LE fluorescence rate increases whereas nonradiative rate decreases with increasing polarity of solvent. In ethylacetate and methanol, lifetime, radiative and nonradiative rate constants are considered to be of average values. Ethylacetate being a solvent of higher polarity compared to dioxane and cyclohexane, decays of both the species are prominent (a_1 = 0.36 and a_2 = 0.64) with longer (838 ps) and the higher abundant component is expected to be because of CT species. In methanol, mostly CT species decays (a_1 = 0.995 and a_2 = 0.005). Methanol being a highly polar hydrogen bonding solvent the more abundant decaying component with lifetime 53.9 ps is for CT species and less abundant component with lifetime 54.8 ps is responsible for LE fluorescence. The longer lifetime of CT species in ethylacetate (838 ps) as compared to that in methanol (53.9 ps) is as a result of lower rates of nonradiative processes because of higher energy difference between CT and triplet states as well as CT and ground states [34] in ethylacetate. This is supported by lesser rates of nonradiative processes and higher quantum yield in ethylacetate as compared to those in methanol (Table 2). The decaying species is absolutely charge transfer in water. Compared to methanol, in water rate of fluorescence decreases and nonradiative rate increases as a result of greater stabilization of charge transfer state in later solvent thereby bringing the state to closer proximity of triplet as well as ground charge transfer states [34]. Theoretical calculations (discussed later) show that the S_5 state is responsible for the polarity induced TICT emission. Since the calculated dipole moment of this S_5^{TICT} state (μ = 17.6 Debye) is much greater than that of the ground singlet TICT state (S_0^{TICT}, μ = 2.76 Debye), the former is much more polar. Therefore, S_5^{TICT} state becomes relatively more stabilized as compared to the S_0^{TICT} state by the influence of the polar medium. This results into a decrease in the energy gap, $\Delta E(S_5^{TICT} - S_0^{TICT})$, with a consequent red shift in the TICT emission. As a result of that the rate of internal conversion from S_5^{TICT} to S_0^{TICT} is higher in water than that in less polar solvents. This fact is in favor of the stronger TICT emission in the less polar medium as compared to that in pure water [29]. Moreover, TICT emissions in less polar solvents are also increased due to the decrease in the rate of intersystem crossing from the S_5^{TICT} state to triplet TICT state [41]. Hydrogen-bonding interaction between 4-DMASP and water is also responsible for fluorescence quenching [34,42] due to radiationless transitions, e.g., in cases of some dyes, stronger hydrogen-bonding solvents have been found to enhance the rate of singlet–triplet intersystem crossing [43]. As a result of that, a weak TICT emission of 4-DMASP is observed in pure water. Slightly lower lifetime of CT species in water (51.5 ps) as compared to that in methanol (53.9 ps) is because of greater stabilization of CT state in water as supported by nonradiative rate constants and quantum yields data (Table 2). The similar explanation is valid for lifetime data in ethylacetate and methanol as discussed above.

3.4. *Effect of hydrogen ion concentration on absorption and fluorescence spectra of 4-DMASP*

There are two basic centers in 4-DMASP, pyridine nitrogen and nitrogen of –N(CH_3)$_2$ group. As mentioned above both absorption and fluorescence spectra show bathochromic shift in hydrogen bonding solvents. Protonation of a molecule is an extreme case of hydrogen bond donating nature of a solvent [18]. Scheme 2 shows equilibrium between different protonated species of 4-DMASP in water as solvent. The absorption and fluorescence peak maxima of neutral species appear at 373 nm and 510 nm, respectively. At a low concentration of hydrogen ions both the bands are red shifted to 447 nm and 610 nm, respectively compared to the bands of neutral species due to the formation of monocation I (Scheme 2). Red shifts of both absorption and fluorescence bands depict that pyridine nitrogen is more basic than nitrogen of –N(CH_3)$_2$ group in ground as well excited states. Monocation I is more stable than the neutral species because of greater extent of transfer of charge from donor to acceptor in this form. The large red shift of the spectrum of monocation I can also be due to the resonance interaction of lone pair of electrons of –N(CH_3)$_2$ group with the π-cloud of acceptor part leading to the resonating structure I′. However, at a high concentration of hydrogen ions dication II is formed due to the protonation of both the nitrogen atoms which results in the blue shift of both absorption and fluorescence bands to 325 nm and 400 nm, respectively compared to the bands corresponding to neutral as

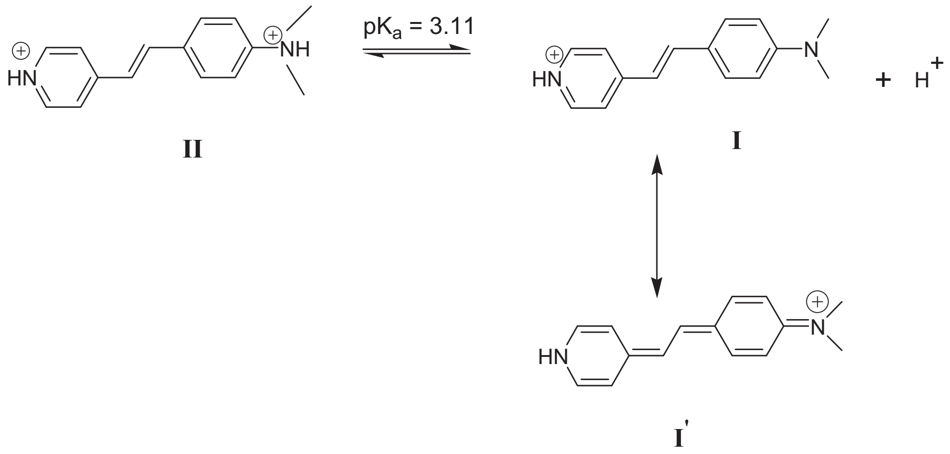

Scheme 2. Equilibrium between dication and monocation of 4-DMASP in aqueous solution.

well as monocation I. This blue shift is because of destabilization of dication II as a result of protection of transfer of charge from donor site due to engagement of lone pair of electrons for protonation. Fig. 7 shows absorption spectra of monocation I and dication II in equilibrium at various pHs. The isosbestic point at 357 nm in the absorption spectra of species I and II reveals the equilibrium present between them. Hence, ground state acidity constant, $\mathrm{p}K_\mathrm{a}$ calculated for this equilibrium is found to be 3.11. Fig. 8 shows fluorescence spectra of both the species (monocation I and dication II) at different pHs of solution. The water Raman peak appears at 408 nm and gets merged with fluorescence band for dication. This Raman peak is as expected obtained for excitation at 357 nm [44] which is an isosbestic point corresponding to dication–monocation equilibrium (Fig. 7). To have a clear view of peak maximum of band corresponding to dication, a fluorescence spectrum has been recorded at excitation wavelength, 325 nm showing peak position at 400 nm and giving Raman peak at 368 nm [Fig. 8 (inset)]. The excited state acidity constant, $\mathrm{p}K_\mathrm{a}^*$ is calculated to be 3.21. Almost same values of ground and excited state acidity constants depict that equilibrium between these two species is not achieved in the excited state as the rate of excited state prototropism is much slower than the rate of deactivation of the lowest excited singlet states by fluorescence [45]. The ground state acidity constant, $\mathrm{p}K_\mathrm{a}$ of monocation I-neutral species equilibrium could not be determined because of not having any clear isosbestic point. The reason for not getting isosbestic point could be because of existence of two resonating structures I and I′ for monocation-I. In case of dication–monocation equilibrium, this problem is less because of protonation of both the nitrogen atoms forming a dication.

3.5. Theoretical calculations

To support the experimental findings of dual characteristics of emission (LE and CT fluorescence), AM1-SCI semi-empirical quantum chemical calculations [24,25,27,46–48] were performed to locate the ground and excited state optimized geometries of 4-DMASP at its various conformations. Experimental results show the presence of intramolecular charge transfer character of 4-DMASP in polar solvents. Hence, to rationalize this behavior theoretically, geometries of 4-DMASP molecule are optimized in the ground and excited states with the torsion angle (ϕ) varying from 0 to 90°. Rotational motions of the donor group, –N(CH_3)$_2$ around the

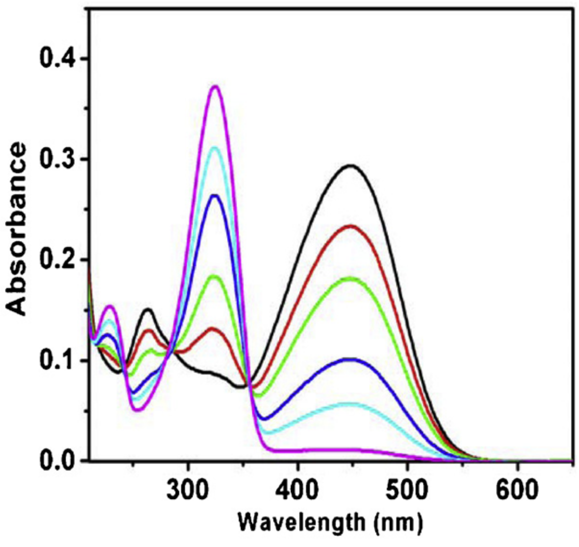

Fig. 7. Absorption spectra of monocation-I and dication-II (Scheme 2) in equilibrium in aqueous solutions of different pHs; 4.0 (⬛), 3.59 (🟥), 3.28 (🟩), 2.9 (🟦), 2.56 (⬜) and 1.86 (🟪). (For interpretation of the references to color in this figure legend, the reader is referred to the web version of the article.)

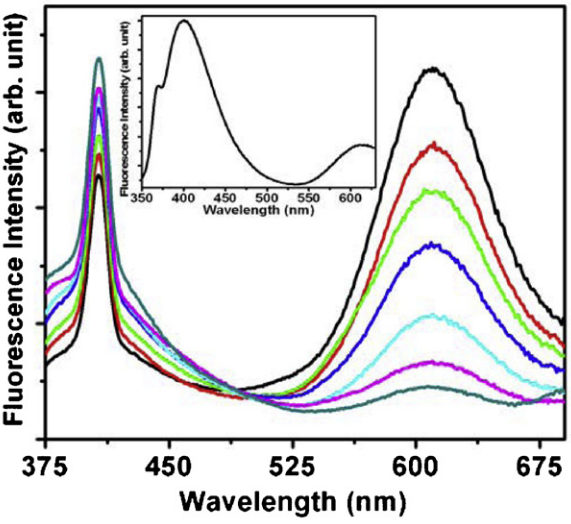

Fig. 8. Emission spectra of 4-DMASP in aqueous solution of different pHs; 3.59 (⬛), 3.39 (🟥), 3.28 (🟩), 3.04 (🟦), 2.90 (⬜), 2.56 (🟪) and 1.86 (🟫) (λ_{ex} = 357 nm). [Inset: fluorescence spectrum of solution of pH = 1.86 at λ_{ex} = 325 nm.] (For interpretation of the references to color in this figure legend, the reader is referred to the web version of the article.)

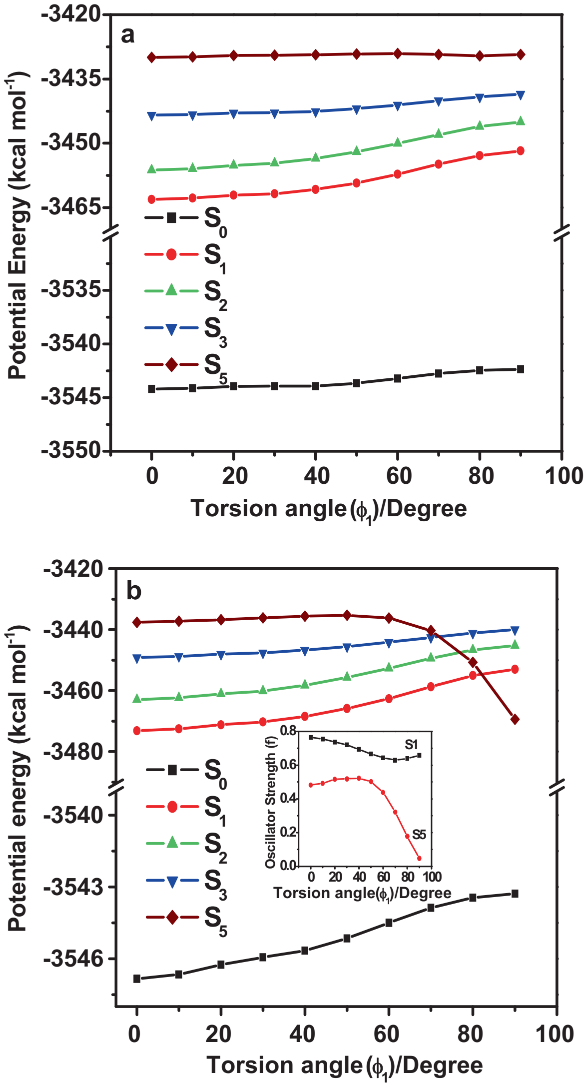

Fig. 9. Variation of potential energy of 4-DMASP in five singlet states with changing torsion angle (11–14–15–16, vide Scheme 1) in (a) vacuo and (b) water. [Inset of (b) represents variation of oscillator strengths in S_1 and S_5 states with changing same torsion angle.]

C14–N15 bond (Scheme 1) and acceptor group around C8–C9 bond are described by the torsion angle, ϕ_1 and ϕ_2, respectively. Potential energy surfaces along the twist coordinate ϕ_1 for ground and several excited states have been determined in vacuo and water as solvent and are plotted in Fig. 9a and b, respectively. Calculation for solvation energy stabilization has been performed using Eq. (2). In vacuo energies of all states increase with increasing torsion angle. However, one can see the significant stabilization of S_5 state at a torsional angle of 90° after carrying out the effect of polar solvent (Fig. 9b represents plot for water as a polar solvent) on the potential energy data obtained from this theoretical calculation. The stabilization of S_5 state below S_1 state is also supported by very high dipole moment value (17.6 Debye) at the same torsional angle (Fig. 10). Hence, the excited state responsible for charge transfer fluorescence in polar solvents can be ascertained to S_5 state whereas LE fluorescence originates from S_1 state. The calculated dipole moment of global minimum structure at ground state is found to be 4.60 Debye with AM1-SCI method. A twisted conformation contributing to increased dipole moment (17.60 Debye) and stabilization of excited state supports the TICT phenomena in polar medium. The charge-transfer transition at a torsional angle of 90° is also reflected by the structure of molecular orbitals and the values of oscillator strength. It can be seen in Fig. 11 that the $S_0 \rightarrow S_1$ transition of planar structure ($\phi_1 = 0°$) is of $\pi \rightarrow \pi^*$ (HOMO → LUMO) character where the lone pair orbital contribution is made through the delocalized feature of HOMO. The $\pi \rightarrow \pi^*$ nature of transition is also supported by high oscillator strength, $f = 0.77$ [Fig. 9b (inset)]. However, $S_0 \rightarrow S_5$ transition of twisted structure ($\phi_1 = 90°$) is of charge-transfer type reflected by its very low value of $f = 0.043$. The low value of f depicts that this charge-transfer transition is forbidden and of $n \rightarrow \pi^*$ type. Nevertheless, HOMO is almost localized lone pair orbital of nitrogen atom of $-N(CH_3)_2$, whereas LUMO is mostly localized at acceptor part of the molecule. A high extent of localization of lone pair on donor nitrogen atom at twisted conformation of the molecule indicates the existence of TICT state [49]. Fig. 12 shows potential energy surfaces along another possible twist coordinate, ϕ_2 at the acceptor side after considering stabilization due to solvation by water molecules. The corresponding potential energy surfaces in vacuo are represented by Figure S2 as supplementary material. In this case also S_5 state gets stabilized at twisted conformation and stabilization is much greater than that in case of donor twisted conformation. Stabilization of S_5 state is also supported by very high value of dipole moment (23.70 Debye) (Figure S3 as supplementary material). However, corresponding HOMO is not at all localized at donor nitrogen atom (Fig. 11c), instead it is quite delocalized over the molecule like planar conformation with global optimized structure. LUMO is different from that at same planar structure with the localization at acceptor side. It indicates that HOMO → LUMO transition ($S_0 \rightarrow S_5$) is a kind of transition from a π orbital to a π orbital of acceptor and it is forbidden supported by very low value of $f = 0.0025$.

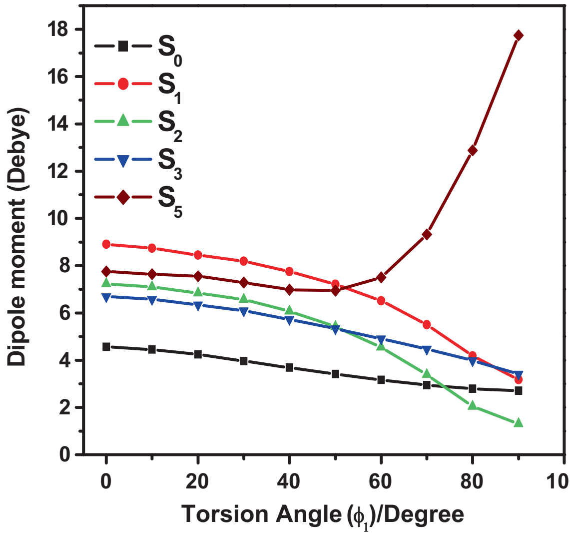

Fig. 10. Variation of dipole moments of 4-DMASP in five singlet states with changing torsion angle (11–14–15–16, vide Scheme 1).

Therefore, theoretical calculation data suggest that the occurrence of large Stokes shifted fluorescence band of 4-DMASP in polar solvent is due to the existence of TICT state through the relaxation of LE state as a result of stabilization of TICT state of large dipole moment. Although, there are possibilities of having charge-transfer states through two different twisted coordinates but unless other supportive data are available and rigorous calculations are carried out, it is difficult to predict the actual path. According to present calculations a path through twisting of donor is more acceptable because of showing lone pair orbital of nitrogen atom of donor as HOMO as required for occurrence of a TICT state [49]. Moreover, closer values of calculated dipole moment (17.60 Debye) of twisted structure with donor twisting angle, $\phi_1 = 90°$ and dipole moment

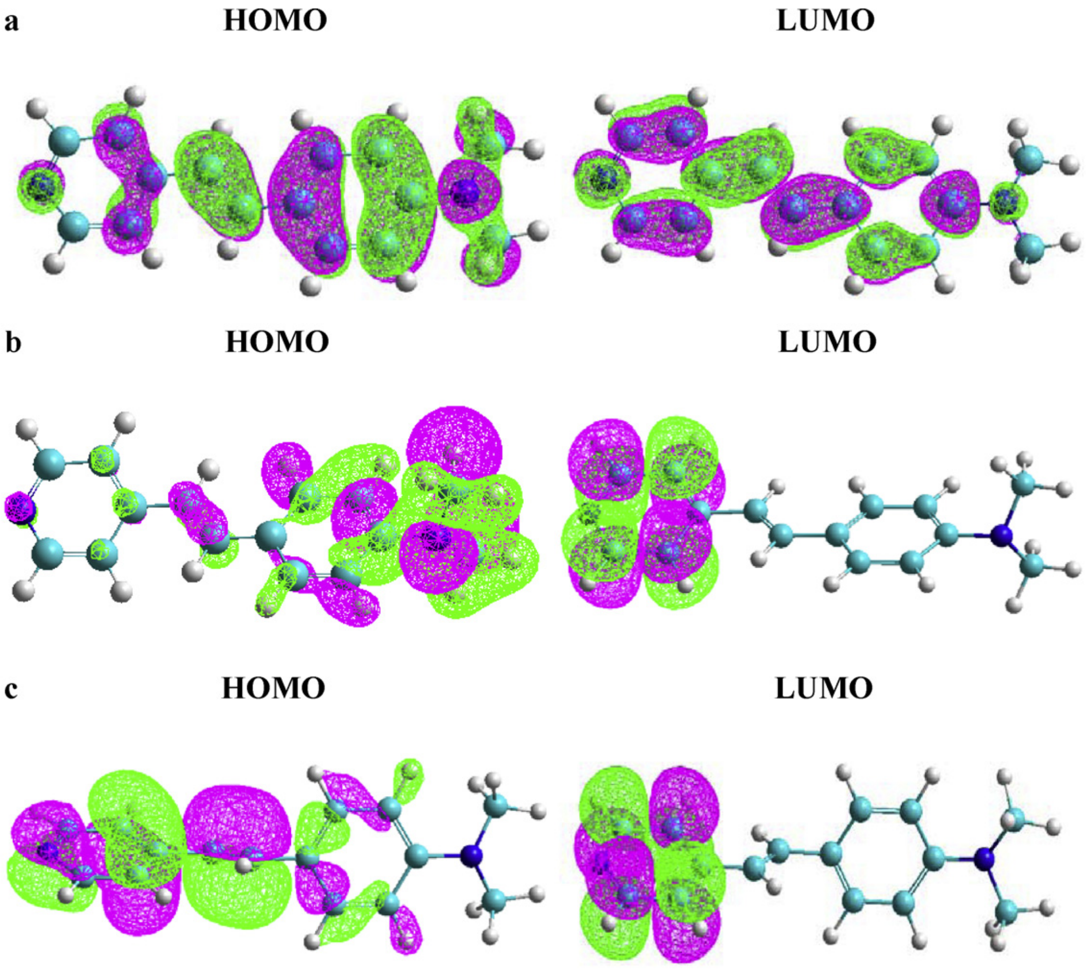

Fig. 11. Frontier molecular orbitals (FMO) of 4-DMASP (a) with planar structure, (b) with twisted donor structure and (c) with twisted acceptor structure.

value obtained from experiment (16.98 Debye) is in favor of donor twisting coordinate as possible path for giving excited TICT state.

Because of similarity of structure of 4-DMASP to that of stilbene derivatives those are well known for their cis–trans photoisomerization [50], configuration interaction calculation using AM1 method has been performed to investigate whether similar kind of isomerization occurring in case of 4-DMASP. This calculation gives the potential energy surface (PES) diagrams (Fig. 13) at different twist angles (22–7–8–23, vide Scheme 1) [47,48]. PES for 4-DMASP in vacuum (solid lines) and those for the solvated (broken line) molecule in dioxane (relative permittivity = 2.22) are shown in the

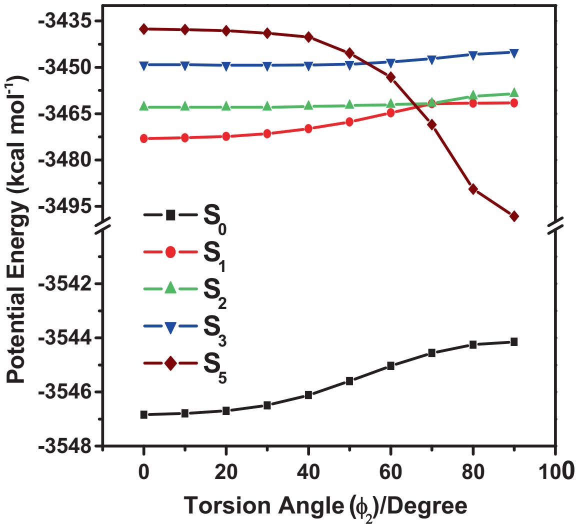

Fig. 12. Variation of potential energy of 4-DMASP in five singlet states with changing torsion angle (7–8–9–10, vide Scheme 1) in water.

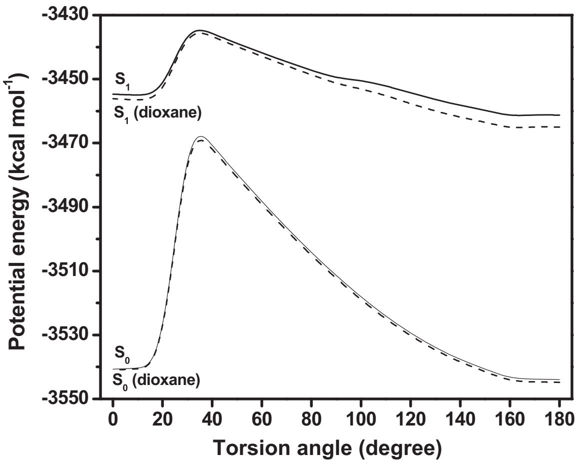

Fig. 13. Configuration interaction calculations using AM1 method showing the potential energy surface (PES) diagram at different twist angles (22–7–8–23, vide Scheme 1).

figure. The figure clearly shows the change in the magnitude of the energy barrier in the ground electronic state (S_0) and first excited singlet state (S_1). In both the states, trans isomer of 4-DMASP is the most stable one. The PES constructed by rotating the aromatic moieties on both sides of the double bond connecting C7 and C8 (vide Scheme 1) clearly shows that the trans geometry is more stable than the cis form in the ground as well as excited states with an energy barrier of 30 kcal mol^{-1} and 76 kcal mol^{-1}, respectively. Since the heat energy supplied at experimental temperature, 25 °C is only 2.8 kcal mol^{-1}, therefore it is expected that neither in the ground state nor in the excited state cis–trans isomerization can occur. Further, study is needed to investigate the photoisomerization at higher temperature. Therefore, it is suggested that unlike stilbene, 4-DMASP retains its trans geometry and shows solvent polarity dependent TICT in the excited state at room temperature. The reason that nonpolar medium (dioxane as solvent) has been chosen to show photoisomerization by PES calculation is to rule out the interference of any TICT in polar medium.

4. Conclusions

Excited states of 4-DMASP are more polar than the ground state. Interactions with hydrogen bond donating solvents offer greater contribution towards the stability of ground state than dipolar interactions. However, dipolar interactions contribute more to the stabilization of an excited state. Such types of interactions contribute more to the stabilization of an excited state than that of ground state. Higher contribution of dipole–dipole interactions towards the stability of excited state in comparison to that of ground state is in accordance with the greater dipole moment of 4-DMASP in the excited state than that in the ground state. The charge density on pyridine nitrogen atom is higher whereas the same on nitrogen atom of –N(CH$_3$)$_2$ group is lower at the excited state compared to that in the ground state as a result of greater extent of flow of charge from donor to acceptor part in the excited state. Emission in a non-polar solvent is originated from the LE state. However, in a polar solvent fluorescence originates from a highly polar CT state. The CT excited state is not only created through rapid relaxation of singly excited LE species giving TICT state but also by the excitation of ground state CT species giving an ICT state. Monoexponential decay in case of a nonpolar solvent is due to a LE species, whereas LE and CT species are responsible for biexponential decay in a polar solvent except in water where charge transfer species only decays. Compared to methanol, rate of fluorescence in water decreases and nonradiative rate increases as a result of greater stabilization of charge transfer state in later solvent thereby becoming closer to triplet as well as ground CT states. Theoretical calculations suggest that S_5 state is responsible for the polarity induced TICT emission. The calculated dipole moment of this S_5^{TICT} state (μ = 17.60 Debye) obtained through the twisted coordinate at donor site is in good agreement with the dipole moment value determined experimentally (μ = 16.98 Debye). Theoretical calculations show that the $S_0 \rightarrow S_1$ transition of planar structure is of $\pi \rightarrow \pi^*$ character (f = 0.77), whereas $S_0 \rightarrow S_5$ transition of twisted ground state structure is of charge-transfer type characterized by $n \rightarrow \pi^*$ transition and supported by its very low value of f = 0.043. A high extent of localization of lone pair on donor nitrogen atom at a twisted conformation obtained through the twisting of donor indicates that donor twisting is a possible path for existence of a TICT state rather than acceptor twisting. Moreover, very good agreement between the dipole moment of twisted structure with donor twisting angle, ϕ_1 = 90° and the experimental dipole moment is also in favor of donor twisting coordinate as possible path for giving excited TICT state. The calculated dipole moment in case of twisted structure with acceptor twisting angle, ϕ_2 = 90° is found to be very high (23.70 Debye) in comparison to experimental value. Pyridine nitrogen is more basic than nitrogen of –N(CH$_3$)$_2$ group in ground state as well as in excited state. The ground state acidity constant, pK_a for dication–monocation equilibrium is calculated to be 3.11. Excited state acidity constant for the same equilibrium could not be calculated as the rate of excited state prototropism is much slower than the rate of deactivation of the lowest excited singlet state by fluorescence. Configuration interaction calculation performed using AM1 method suggests that neither in the ground state nor in the excited state cis–trans isomerization can occur at room temperature.

Acknowledgements

SKS acknowledges the University Grants Commission for financial supports under major research project (33-257/2007(SR)) and special assistance programme (F.540/14/DRS/2007 (SAP-I) and the Council of Scientific and Industrial Research (CSIR) for financial supports under major research project (01(2213)08/EMR-II), Govt. of India. MS acknowledges CSIR for financial support under senior research fellowship. We also extend our acknowledgement to The Laser Spectra Services, Bangalore for allowing us to use the time-correlated single photon counting setup.

Appendix A. Supplementary data

Supplementary data associated with this article can be found, in the online version, at doi:10.1016/j.jphotochem.2010.12.006.

References

[1] K. Rotkiewicz, K.H. Grellmann, Z.R. Grabowski, Chem. Phys. Lett. 19 (1973) 315–318.

[2] Z.R. Grabowski, K. Rotkiewicz, A. Siemiarczuk, D.J. Cowley, W. Baumann, Nouv. J. Chim. 3 (1979) 443–454.

[3] W. Tan, D. Zhanga, D. Zhua, Bioorg. Med. Chem. Lett. 17 (2007) 2629–2633.

[4] A. Mielniczak, B. Wandelt, S. Wysocki, Mater. Sci. 20 (2002) 59–69.

[5] S.S. Jaffer, S.K. Saha, P. Purkayastha, J. Colloid Interface Sci. 337 (2009) 294–299.

[6] G. Krishnamoorthy, S.K. Dogra, Spectrochim. Acta A 55 (1999) 2647–2658.

[7] M. Maus, Photoinduced Intramolecular Charge Transfer in Donor–Acceptor Biaryls and Resulting Applicational Aspects Regarding Fluorescent Probe and Solar Energy Conversion, Universal Publishers, USA, 1998.

[8] Z.R. Grabowski, Pure Appl. Chem. 64 (1992) 1249–1255.

[9] W. Rettig, Angew. Chem. Int. Ed. Engl. 25 (1986) 971–988.

[10] J. Herbich, Z.R. Grabowski, H. Wojtowicz, K.J. Golankiewicz, Phys. Chem. 93 (1989) 3439–3444.

[11] K. Bhattacharyya, M. Chowdhury, Chem. Rev. 93 (1993) 507–535.

[12] H. Itagaki, K. Horie, I. Mita, Prog. Polym. Sci. 15 (1990) 361–424.

[13] B. Wandelt, P. Turkewitsch, B.R. Stranix, G.D. Darling, J. Chem. Soc. Faraday Trans. 91 (1995) 4199–4205.

[14] B. Wandlet, A. Mielniczak, P. Turkewitsch, G.D. Darling, B.R. Stranix, Biosens. Bioelectron. 18 (2003) 465–471.

[15] C.-Y. Chen, J.-H. Ho, S.-L. Wang, T.-I. Ho, Photochem. Photobiol. Sci. 2 (2003) 1232–1236.

[16] D. Jozwik, E. Miller, B. Wandelt, S. Wysocki, Spectrochim. Acta A 64 (2006) 1125–1132.

[17] S. Bruni, E. Cariati, F. Cariati, F.A. Porta, S. Quici, D. Roberto, Spectrochim. Acta A 57 (2001) 1417–1426.

[18] S.-L. Wang, G.-Y. Gao, T.-I. Ho, L.-Y. Yang, Chem. Phys. Lett. 415 (2005) 217–222.

[19] A. Chakraborty, S. Kar, N. Guchhait, J. Photochem. Photobiol. A: Chem. 181 (2006) 246–256.

[20] M.J. Kamlet, J.-L.M. Abboud, M.H. Abraham, R.W. Taft, J. Org. Chem. 48 (1983) 2877–2887.

[21] M.J.S. Dewar, E.G. Zoebisch, E.F. Healy, J.J.P. Stewart, J. Am. Chem. Soc. 107 (1985) 3902–3909.

[22] M.J.S. Dewar, K.M. Dieter, J. Am. Chem. Soc. 108 (1986) 8075–8086.

[23] J.J.P. Stewart, J. Comput.-Aided Mol. Des. 4 (1990) 1–105.

[24] J.J.P. Stewart, J. Comput. Chem. 10 (1989) 209–220.

[25] C.J.F. Bottcher, Theory of Electronic Polarization, vol. 1, Elsevier, Amsterdam, 1983.

[26] T. Kobayashi, M. Futakami, O. Kajimoto, Chem. Phys. Lett. 141 (1987) 450–454.

[27] S.K. Saha, P. Purkayastha, A.B. Das, J. Photochem. Photobiol. A: Chem. 195 (2008) 368–377.

[28] M.-J. Frish, G.W. Trucks, H.B. Schlegel, G.E. Scuseria, M.A. Robb, J.R. Cheeseman, et al., Gaussian 98 Revision A.7, Gaussian, Inc., Pittsburgh, PA, 1998.

[29] A. Mallick, S. Maiti, B. Haldar, P. Purkayastha, N. Chattopadhyay, Chem. Phys. Lett. 371 (2003) 688–693.

[30] N. Ghoneim, P. Suppan, Pure Appl. Chem. 65 (1993) 1739–1743.

[31] C. Reichardt, Solvent Effects in Organic Chemistry, Weinheim, 1979.
[32] H. Gusten, R. Maisner, J. Photochem. 21 (1983) 53–60.
[33] A. Ray, Nature 231 (1971) 313–315.
[34] R. Das, D. Guha, S. Mitra, S. Kar, S. Lahiri, S. Mukherjee, J. Phys. Chem. A 101 (1997) 4042–4047.
[35] B. Albinsson, J. Am. Chem. Soc. 119 (1997) 6369–6375.
[36] A.L. Sobolewski, W. Domcke, Chem. Phys. Lett. 250 (1996) 428–436.
[37] F.D. Lewis, J.-S. Yang, J. Am. Chem. Soc. 119 (1997) 3834–3835.
[38] E. Lippert, Z. Naturforsch. A 10 (1955) 541.
[39] P.R. Bangal, S. Panja, S. Chakravorti, J. Photochem. Photobiol. A: Chem. 139 (2001) 5–16.
[40] A. Mallick, B. Haldar, N. Chattopadhyay, J. Phys. Chem. B 109 (2005) 14683–14690.
[41] P. Avouris, W.M. Gelbert, M.A. El-Sayed, Chem. Rev. 77 (1977) 793–833.
[42] L.E. Cramer, K.G. Spears, J. Am. Chem. Soc. 100 (1978) 221–227.
[43] S. Swaminathan, S.K. Dogra, J. Am. Chem. Soc. 105 (1983) 6223–6228.
[44] J.R. Lakowicz, Principles of Fluorescence Spectroscopy, Kluwer Academic, New York, 1999.
[45] S.G. Schulman, Fluorescence and Phosphorescence Spectroscopy: Physicochemical Principles and Practice, Pergamon Press, New York, 1977.
[46] A.-D. Gorse, M. Pesquer, J. Phys. Chem. 99 (1995) 4039–4049.
[47] P. Purkayastha, N. Chattopadhyay, Phys. Chem. Chem. Phys. 2 (2000) 203–210.
[48] P. Purkayastha, N. Chattopadhyay, Int. J. Mol. Sci. 4 (2003) 335–361.
[49] Z. Grabowski, K. Rotkiewicz, W. Rettig, Chem. Rev. 103 (2003) 3899–4032.
[50] S. Arzhantsev, K.A. Zachariasse, M. Maroncelli, J. Phys. Chem. A 110 (2006) 3454–3470.